ISSN 1674-1056
http://cpb.iphy.ac.cn
http://iopscience.iop.org/cpb
中国物理 B
Chinese Physics
中国物理 Chinese Physics B

Tracking coherent low frequency vibrational information of Rhodamine101 in ground and excited electronic states by broadband transient grating spectroscopy

Wei Zhang(张伟), Xiao-Song Liu(刘小嵩), Zan-Hao Wang(王赞浩), Yun-Fei Song(宋云飞), Yan-Qiang Yang(杨延强)

Citation: Chin. Phys. B . 2018, 27(12): 123301. **doi:** 10.1088/1674-1056/27/12/123301
Journal homepage: http://cpb.iphy.ac.cn; http://iopscience.iop.org/cpb

What follows is a list of articles you may be interested in

Photoassociation spectra of ultracold $^{85}Rb_2$ molecule in 0_u^+ long range state near the $5S_{1/2}+5P_{1/2}$asymptote

Guodong Zhao(赵国栋), Dianqiang Su(苏殿强), Zhonghua Ji(姬中华), Tengfei Meng(孟腾飞), Yanting Zhao(赵延霆), Liantuan Xiao(肖连团), Suotang Jia(贾锁堂)

Chin. Phys. B . 2017, 26(8): 083301. **doi:** 10.1088/1674-1056/26/8/083301

Study on the $A^2\Pi_{3/2u}$, $B^2\Delta_{3/2u}$, and $X^2\Pi_{3/2g}$ states of Cl_2^+ including its isotopologues

Wu Ling, You Su-Ping, Shao Xu-Ping, Chen Gang-Jin, Ding Ning, Wang You-Mei, Yang Xiao-Hua

Chin. Phys. B . 2015, 24(8): 083301. **doi:** 10.1088/1674-1056/24/8/083301

Infrared diode laser spectroscopy of O_2–N_2O van der Waals complex in the v_1 symmetric stretch region of N_2O

Li Song, Zheng Rui, Duan Chuan-Xi

Chin. Phys. B . 2014, 23(12): 123301. **doi:** 10.1088/1674-1056/23/12/123301

The structural and spectroscopic properties for uranium oxides

Li Peng,Jia Ting-Ting,Gao Tao,Li Gan

Chin. Phys. B . 2012, 21(4): 043301. **doi:** 10.1088/1674-1056/21/4/043301

P-branch emission spectra of the $A^1\Pi$–$X^1\Sigma^+$ system of IrN

Fan Qun-Chao,Sun Wei-Guo,Li Hui-Dong,Feng Hao

Chin. Phys. B . 2012, 21(2): 023301. **doi:** 10.1088/1674-1056/21/2/023301

Tracking coherent low frequency vibrational information of Rh101 in ground and excited electronic states by broadband transient grating spectroscopy*

Wei Zhang(张伟)[1], Xiao-Song Liu(刘小嵩)[1], Zan-Hao Wang(王赞浩)[1], Yun-Fei Song(宋云飞)[2], and Yan-Qiang Yang(杨延强)[1,2,†]

[1] *Department of Physics, Harbin Institute of Technology, Harbin* 150001, *China*
[2] *National Key Laboratory of Shock Wave and Detonation Physics, Institute of Fluid Physics, China Academy of Engineering Physics, Mianyang* 621900, *China*

(Received 17 April 2018; revised manuscript received 28 September 2018; published online 10 November 2018)

Time- and frequency-resolved broadband transient grating (BB-TG) spectroscopy is used to distinguish between ground- and excite-electronic state vibrational coherence at different wavelengths. Qualitative theoretical analysis using double-sided Feynman diagrams indicates that a superposition of ground and excited state vibrational coherence are contained in the ground state absorption (GSA) and stimulated emission (SE) overlap band, while only the excited state is contained in the excited state absorption (ESA) band. The TG experiment, in which a white light continuum (WLC) is adopted as a probe, is conducted with rhodamine101 ($Rh101^{+}$) as the target molecule. Fourier analysis of TG dynamics in a positive delay time range at specific wavelengths enables us to distinguish the low-frequency vibrational modes of Rh101 in ground- and excite-electronic states.

Keywords: transient grating, Rh101, low-frequency Raman, vibrational spectrum

PACS: 33.15.Mt, 33.20.Tp, 33.20.-t, 36.20.Ng **DOI:** 10.1088/1674-1056/27/12/123301

1. Introduction

At a molecular level, the coherence and relaxation of vibrations play an important role in chemical reactions, both in the electronic ground state and in the excited state (which are named ground state and excited state hereafter). The research on the vibrational coherence of specific molecules is helpful to enhance the cognition of vibrational evolution during electronic transition, tracing the chemical reaction path,[1] and even designing and manufacturing photo-switches, and to some extent molecular machines.[2–4]

A direct method to obtain the vibrational information of a given molecule in different electronic states is to measure its frequency domain; *i.e.*, off-resonant combination with resonant Raman technique.[5] However, low-frequency vibrational modes ($< 100\ cm^{-1}$) are difficult to observe in the frequency domain in liquid ambient due to the intense Rayleigh wing. Furthermore, like laser dyes, the electronic excited state vibrations of a molecule are very difficult to distinguish in the frequency domain due to their strong fluorescence.

In recent years, with the advent of a femtosecond laser[6] whose pulse duration is shorter than plentiful photochemical and photophysical processes, the evolution of specific vibrational wavepackets in ground and electronic excited states can be traced and monitored in the time domain. The molecular vibrational modes, even with low frequency, can be obtained via Fourier transform (FT). In addition, the time domain measurement is immune to the fluorescence noise in excited states. A large number of studies[7–13] have proven its feasibility and two main methods have been established to distinguish vibrational coherence from different electronic states. The first method is Fourier analysis for different time periods of the dynamics, to be specific, positive (probe pulse goes after pump pulse in time) and negative (probe preceding pump pulse) periods. Kiefer and coworkers[9] used iodine vapor as a model molecule and studied the dynamics in different time ranges by using coherent anti-Stokes Raman scattering (CARS) technique with the pump and probe pulses resonant with the sample. Their results indicated that for the negative range, the CARS transient revealed the dynamics of the excited state of iodine; while for positive delay time, both the ground state and excited state dynamics were probed.[7,9] In addition, coherent Stokes Raman scattering (CSRS),[9] four-wave mixing (FWM)[9,12] and transient grating (TG)[8,14] technique were also discussed to separate electronic ground state vibrational dynamics in the same way as the excited state. To obtain a more precise excited state vibrational frequency, a relatively long period of transient in negative delay time range is needed. Meanwhile, the broadband transient absorption (TA)

*Project supported by the Science Challenge Project, China (Grant No. TZ2016001) and the National Natural Science Foundation of China (Grant No. 21673211).

†Corresponding author. E-mail: yqyang@hit.edu.cn

© 2018 Chinese Physical Society and IOP Publishing Ltd

technique has also been employed to study the dynamics and vibrational coherence of different molecules. The dynamics of an excited state can be distinguished from ground state similarly.[10,11]

The other method is broadband impulsive vibrational spectroscopy (BB-IVS), which was established by Kukura *et al.*[13] Their approach was based on impulsive stimulated Raman scattering (ISRS),[15] and simply used a sufficiently short laser pulse whose time duration is shorter than the vibration period to exert an impulsive driving force to coherently stimulate corresponding vibration modes.[16] They combined the off-resonant ultrashort impulsive pulse with a time delayed uncompressed white light continuum (WLC) probe to record ground state vibrational coherences in the time domain.[17] If there is an actinic laser that is resonant with the sample molecule stimulated mixture of ground- and excited-state molecules before the impulsive pulse, then both ground- and excited-state vibrational coherence can be traced.[18] However, the excited-state vibrational modes are mixed up with those in the ground state, which makes it difficult to distinguish the vibrational information from different states.

Although both of these methods can detect vibrational coherences in different electronic states, each has limitations. In particular, the vibrational frequency obtained by first method is of low accuracy due to the short electronic dephasing time.[10] While for the second method, at least two experiments are needed to distinguish the vibration information from different electronic states.

In the present research, the BB-TG technique is adopted to detect the vibrational coherence in different electronic states. The direction of TG signal is separated from the direction of the pump and probe light, so the technique can realize 'back-ground free detection,' which gives rise to an extremely high signal-to-noise ratio. A WLC is used as the probe light, which can cover broadband spectral range, so the dynamic properties of different electronic states can be detected at different wavelengths. In virtue of broadband frequency coverage and accurate time resolution, only one measurement in positive delay time is needed to differentiate the vibrational coherence of ground-state from that of excited-state. Compared with the previously mentioned methods, the BB-TG technique provides a concise and effective way to investigate the vibrational information of specific molecules.

2. Theoretical background

The TG is an FWM technique that is often employed to study molecular dynamics. The time sequence and beam configuration of pump and probe light are exhibited in Figs. 1(a) and 1(b), respectively. Two parallel laser beams were overlapped temporally and spatially in a sample to create a grating. Afterwards, the grating area in the sample was detected by a time-scanned probe pulse, as shown by $\boldsymbol{E}_{\rm c}$ in Fig. 1(a), and the TG signal that carries molecular dynamical information appears in the phase-matching direction. If the spectral width of probe pulse is broad enough, then the dynamic behavior for the stimulated emission (SE), ground state absorption (GSA) and excited state absorption (ESA) can be detected simultaneously.

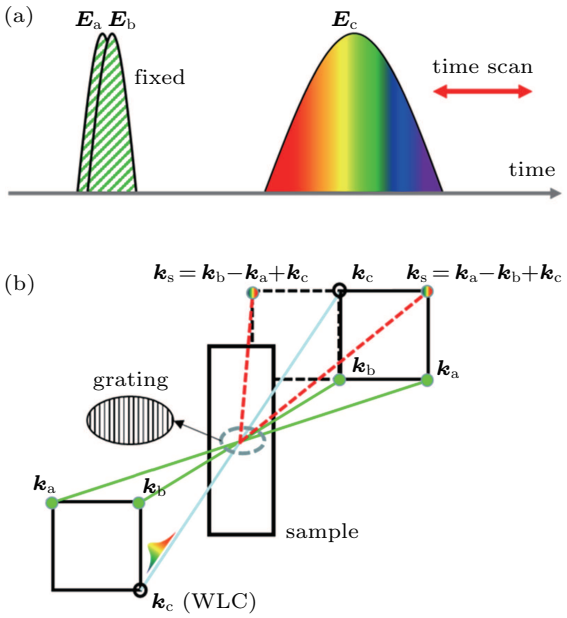


Fig. 1. (color online) (a) Time sequence of the pump and probe pulse, where two pump pulses are fixed in time while probe is of time scanning. (b) Beam configuration of pump, probe, and TG signal in TG measurement.

There are several beam configurations that can be adopted to realize TG measurement. In this study, forward folded BOXCARS[19] arrangement is chosen, as shown in Fig. 1(b) according to its better temporal and spectral resolution. The TG signal appear in the direction of $\boldsymbol{k}_{\rm s} = \boldsymbol{k}_{\rm a} - \boldsymbol{k}_{\rm b} + \boldsymbol{k}_{\rm c}$ and $\boldsymbol{k}_{\rm s} = \boldsymbol{k}_{\rm b} - \boldsymbol{k}_{\rm a} + \boldsymbol{k}_{\rm c}$. In this work, TG signal that appears in the $\boldsymbol{k}_{\rm s} = \boldsymbol{k}_{\rm a} - \boldsymbol{k}_{\rm b} + \boldsymbol{k}_{\rm c}$ direction is collected.

The TG signal intensity ($I_{\rm TG}$) that results from the interaction between three incident laser pulses and sample medium can be estimated from[20]

$$I_{\rm TG} = \int_{-\infty}^{\infty} \left| \boldsymbol{P}^{(3)}(\boldsymbol{k}_{\rm s}, t) \right|^2 {\rm d}t,$$

where $\boldsymbol{P}^{(3)}(\boldsymbol{k}_{\rm s}, t)$ represents the time-dependent third-order polarization under a specific phase matching condition. This equation is applicable for the homodyne detection. For the TG measurements in this research, $\boldsymbol{P}^{(3)}(\boldsymbol{k}_{\rm s}, t)$ can be defined as[20,21]

$$\begin{aligned} \boldsymbol{P}^{(3)}(\boldsymbol{k}_{\rm s}, t) &= -\boldsymbol{E}{\rm b}(t) \int_0^{\infty} \left| \boldsymbol{E}_{\rm a}(\tau - t') \right|^2 \boldsymbol{\chi}^{(3)}(t') {\rm d}t' \\ &= {\rm Tr}\left[\hat{\boldsymbol{P}} \hat{\boldsymbol{\rho}}^{(3)}(t) \right], \end{aligned}$$

where $\boldsymbol{\chi}^{(3)}(t)$ is the third order susceptibility associated with the system, $\boldsymbol{E}_{\rm a}$ and $\boldsymbol{E}_{\rm b}$ are the electric field of the pulses form-

ing the TG and the electric field that scatters from the TG, respectively, $\hat{\boldsymbol{P}}$ represents the polarization, and $\hat{\rho}^{(3)}(t)$ denotes the third-order density operator of the signal.

The evolution of the system under the influence of the incident electromagnetic field and the intrinsic relaxation process can be described by $\hat{\rho}^{(3)}(t)$. The explicit form of $\hat{\rho}^{(3)}(t)$ can be analyzed and illustrated schematically by double-sided Feynman diagrams.[8,21] Dantus *et al.*[8] described the double-sided Feynman diagrams in detail in the TG measurement based on the near-resonant condition. In the rotating wave approximation (RWA), only eight diagrams could make obvious contribution to the third-susceptibility[8] according to the time sequence of probe pulse $\boldsymbol{E}_{\rm c}$ with two pump pulses $\boldsymbol{E}_{\rm a}$ and $\boldsymbol{E}_{\rm b}$. However, the ESA band in positive delay time range was not considered in their work.

In this research, GSA, SE, and ESA bands in positive delay time range of TG measurement were all considered. Six possible diagrams were involved to describe the TG signal under RWA: four are applicable to SE & GSA overlapping band while the other two hold true in ESA process. The four diagrams shown in Figs. 2(a) and 2(b) represent ground state and excited state dynamics respectively, and have been analyzed by Dantus *et al.*[8,21] In particular, in the GSA scheme as shown in Fig. 2(a), after $\boldsymbol{E}_{\rm a}$ and $\boldsymbol{E}_{\rm b}$ interacted with the system, the transform of $\rho_{gg}^{(0)}$ into $\rho_{g'g}^{(2)}$ and $\rho_{gg'}^{(2)}$ occurred. Ground state dynamics could be obtained after $\boldsymbol{E}_{\rm c}$ has scattered from the grating. Another case could also be formed in Fig. 2(b), that $\boldsymbol{E}_{\rm a}$ and $\boldsymbol{E}_{\rm b}$ gave rise to the transform of $\rho_{gg}^{(0)}$ into $\rho_{e'e}^{(2)}$ and $\rho_{ee'}^{(2)}$, excited state dynamics can be traced in time domain after $\boldsymbol{E}_{\rm c}$ has scattered from the grating. Hence, the overlapping band in spectrum contains a superposition dynamics of ground and excited state.

The homologous diagrams for the ESA band are shown in Fig. 2(c). Because the vibrational levels in high excited state e_2 were taken into account, the first excited state vibrational levels were written as e_1 and e_1'. The first two pulses $\boldsymbol{E}_{\rm a}$ and $\boldsymbol{E}_{\rm b}$ made the density operator turn into $\rho_{e_1'e_1}^{(2)}$ and $\rho_{e_1e_1'}^{(2)}$, If the broadband probe pulse has components that are resonant with ESA band of the sample, then after interacting with the system, the density operator will further transform into $\rho_{e_2e_1}^{(3)}$ and $\rho_{e_2e_1'}^{(3)}$, respectively. Therefore, only first excited state dynamics were detected by the probe pulse $\boldsymbol{E}_{\rm c}$ in the ESA band. In brief, if the SE & GSA and ESA band of a certain sample are not overlapped in the spectrum, then the vibrational coherence in ground state and excited state can be distinguished in positive delay time range by different wavelengths.

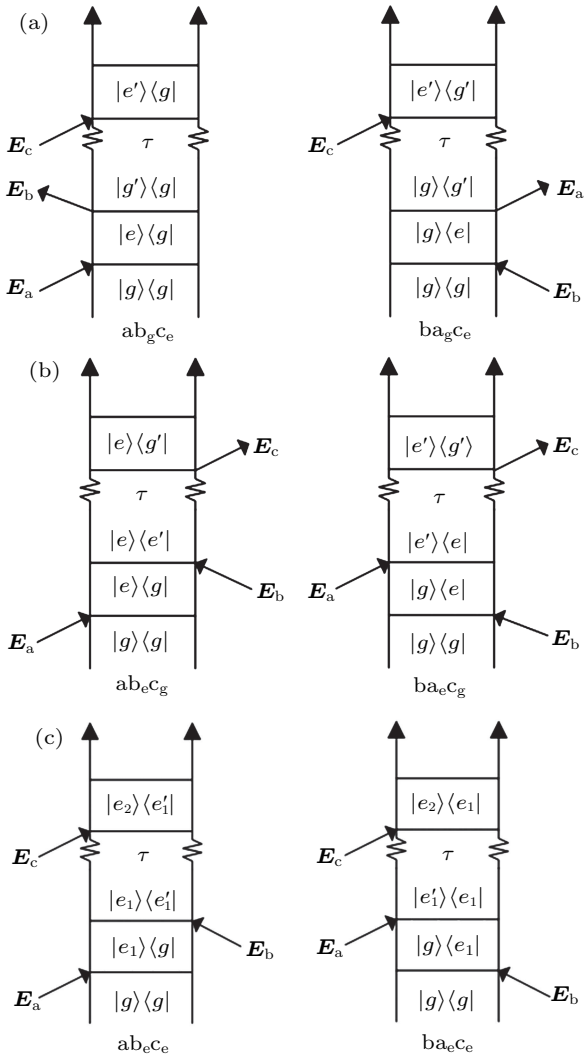


Fig. 2. Double-sided Feynman diagrams corresponding to (a) GSA, (b) SE, and (c) ESA of TG in positive delay time range, where $E_{\rm a}$ and $E_{\rm b}$ denote pump pulses while $E_{\rm c}$ presents probe pulse.

3. Experiment

Rhodamine101 (Rh101) was purchased from Sigma–Aldrich and the molecular skeleton is shown in the inset of Fig. 3(a). The sample was dissolved in methanol (MEOH) with a concentration of 0.1 mmol/L in all the experimental research (Rh101 would exist in the form of cation in MEOH). Inter-molecular electron transfer and proton transfer did not occur between $\mathrm{Rh101}^{+}$ and solvent on account of the inertia of the MEOH. The MEOH was of analytical reagent grade and directly used without further purification.

Steady-state absorption spectrum was measured with an UV–Vis spectrophotometer (720 PC, Shanghai). Steady-state fluorescence spectrum upon excitation by a 532-nm femtosecond laser was recorded with a spectrometer (Chromex 500IS/SM, BRUKER) and CCD (DU440, Andor).

The TG measurement step has been reported previously.[22] Briefly, the 800-nm, 110-fs pulse duration, 1-kHz repetition output pulse was split into two beams by a 9:1 beam splitter. The 90% beam pumped an optical paramet-

ric amplifier (OPA, OPA-800FC, Spectra Physics) to produce a pulse with a central wavelength of 532 nm, which was split into two uniform beams. The energy of each pulse is 0.3 μJ. These beams that are resonant with the sample were used as the pump light in the TG experiment. Because the bandwidth of femtosecond pump pulse was about 10 nm, the coherent vibrational modes with low frequency could be stimulated coherently through impulsive stimulated Raman scattering.[23]

The other 10% beam was focused onto water to produce a WLC, which was used as the probe light. Its spectral range could cover the entire visible region. The probe light went through the optical delay line (ODL) and superposed with the two pump beams in the sample spatially. The TG signal appeared in the direction of the phase-matching condition and was transmitted to the spectrometer and measured by a thermoelectrically cooled charge coupled device (CCD) (DU440, Andor). The stepping motor in the ODL moved in steps of 62.5 fs to give time-resolved TG spectra. All of the experiments were carried out at room temperature in a dark room.

4. Results and discussion

To verify the dynamical information at different wavelengths in time-resolved BB-TG spectrum, the steady-state UV-Vis absorption spectrum and fluorescence spectrum of Rh101$^+$/MEOH (mixed solution) are measured. The normalized steady-state absorption spectrum and the fluorescence spectrum (excited at 532 nm) of the sample are shown in Fig. 3(a). The absorption curve is featured by a peak located at 566 nm and a vibronic shoulder[24] at about 530 nm. The fluorescence spectrum is mirror symmetrical to the absorption spectrum with a peak at 592 nm and a shoulder near 640 nm.

The excited state lifetime of Rh101$^+$ in methanol is about 4 ns,[25,26] basically, the intensity of TG spectrum has slight change in our detecting time window (tens of ps). Typical TG spectrum is shown in Fig. 3(b), the broad band around 480 nm–550 nm corresponds to the steady-state absorption GSA of Rh101$^+$, the band with a peak located around 590 nm stems from SE of Rh101$^+$∗. The peak at 460 nm originates from the ESA of Rh101$^+$∗.[27]

The high frequency vibrational modes of Rh101 have been discussed before by experimental measurement and calculation.[17,28] Moreover, due to limitation of the pump pulse duration of 110 fs, only components with a period longer than 220 fs (frequency less than 150 cm^{-1}) can be distinguished efficiently according to the Nyquist sampling theory. So, we only focus on the low-frequency portion of the TG spectrum in the following analysis. For the solvent, the lowest frequency vibration mode of MEOH is larger than 400 cm^{-1}, which will not obstruct the identification of low-frequency modes of Rh101$^+$ in FT power spectra.

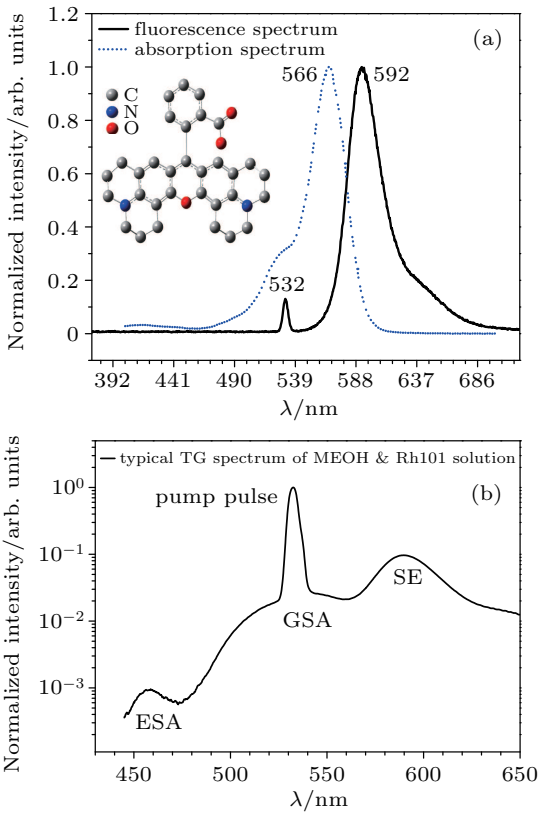


Fig. 3. (color online) (a) Normalized steady-state absorption (dashed curve) and fluorescence spectrum of Rh101$^+$/MEOH, where inset shows molecular skeleton of Rh101; (b) typical TG spectrum of Rh101$^+$/MEOH measured upon excitation at 532 nm. ESA band and GSA band as well as SE band can be observed in this spectrum.

The TG transient in SE & GSA overlap band (585 nm) and ESA band (460 nm) is shown in Fig. 4. The coherent vibrational information of Rh101$^+$ in different electronic sates is contained in the time varying oscillating curves. On the basis of theoretical analysis in the theoretical section above, the measured TG dynamics evolution at 460 nm should contain electronic excited state vibrational information of the Rh101$^+$, while dynamics at 585 nm should contain both ground- and excited- electronic state vibrational information.

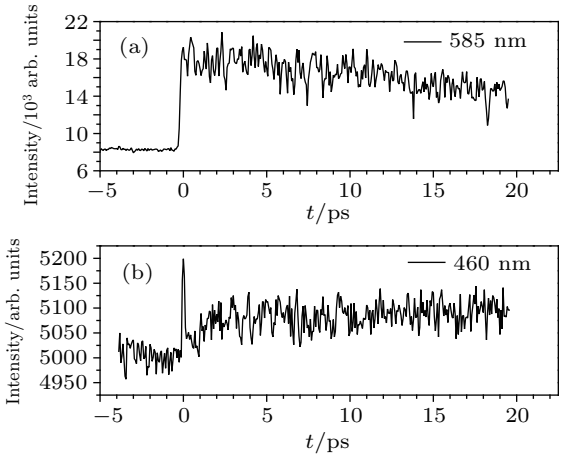


Fig. 4. TG transient of Rh101$^+$/MEOH in (a) GSA & SE overlap band and (b) ESA band.

The FT power spectra of the TG signal at 460 nm and 585 nm in positive range are shown in Figs. 5(a) and 5(b), with a resolution of about ± 2.9 cm^{-1}. The peaks that emerged represent vibrational modes in ground (S_0) and excited (S_1) electronic states. However, it is scarcely possible to identify each vibrational mode only from the FT spectra.

To identify the vibrational coherence in different electronic states, the quantum chemical calculation program Gaussian 03[29] is adopted. The minimum energy point configuration of ground and first electronic excited states of $Rh101^+$ radical cation are optimized by the density functional theory (DFT) and TD-DFT B3LYP method with the "6-311+G (d, p)" basis set. The solvent effect is treated by the polarizable continuum model (PCM), methanol is chosen as the solvent to keep consistent with the experiment. The calculated Raman frequencies of $Rh101^+$ in ground state and excited state are not scaled in this work because the Raman scaled factor was not suited for all of the vibrational modes.[30,31] Moreover, a few percent correction has little influence on low-frequency modes that are under 100 cm^{-1}.

The calculated vibrational modes of $Rh101^+$ in S_1 and S_0 states are shown in Figs. 5(c) and 5(d), respectively. To more clearly illustrate the vibrations of two electronic states, the theoretical and experimental results of low frequencies and their assignments are listed in Table 1.

The experimental results are consistent with theoretical expectations. In Figs. 5(a) and 5(b), almost all of the peaks in FT power spectra of ESA band (460 nm) also appear in the GSA & SE band (585 nm) FT power spectrum, as denoted by vertical dotted lines connecting the peaks in Fig. 5(a) and the peaks in Fig. 5(b). These peaks located at 34, 40, 57, and 77 cm^{-1} in Fig. 5(a) are derived from vibrations in S_1 state of $Rh101^+$. The modes only appearing in the GSA & SE overlap band FT power spectrum represent the vibrations of ground state, such as the peaks that are located at 26, 49, and 71 cm^{-1}.

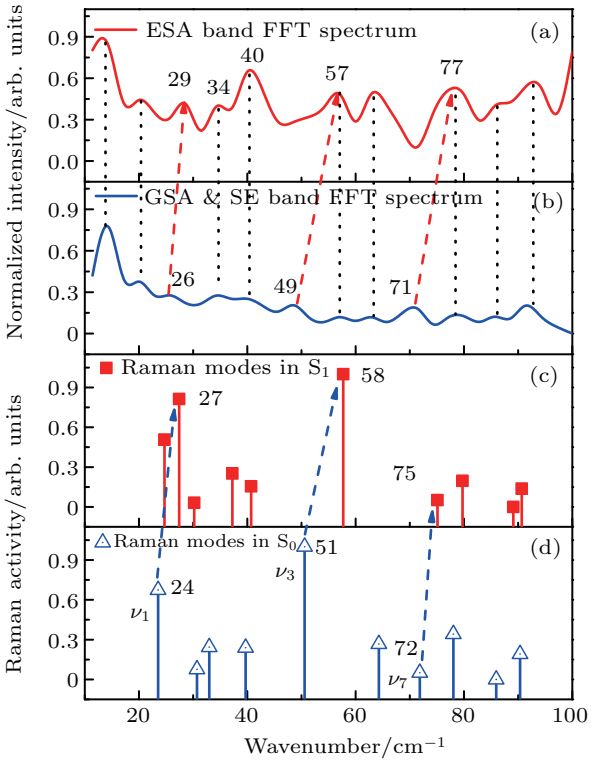


Fig. 5. (color online) (color online) Fourier transform power spectra in (a) ESA band-460 nm and (b) GSA & SE band-585 nm; Gaussian calculated Raman modes in minimum structure of (c) S_1 state and (d) S_0 state. Black-dotted lines connecting panels (a) and (b) represent the same vibrational modes. Dashed-blue arrows pointing to panel (c) from panel (d) denote calculated same vibrational mode blue shift from electronic ground state to excited state while the dashed red arrows refer to the corresponding experimental results.

Table 1. Vibrational modes of $Rh101^+$ in S_0 and S_1 states and their assignments based on calculations.

Mode	S_0 geometry/cm^{-1}		S_1 geometry/cm^{-1}		Assignment
	Theor.	Exp.	Theor.	Exp.	
ν_1	24	26	27	29	Phenyl torsion
ν_2	31	–	30	–	Xanthene ring skeletal bending
ν_3	33	34	41	40	Phenyl wag vertical to xanthene and xanthene skeletal bending
ν_4	40	40	38	34	Xanthene skeletal twist
ν_5	51	49	58	57	Phenyl ring wag parallel with xanthene
ν_6	64	63	25	25	Carboxyl group torsion and CH_2 twist
ν_7	72	71	75	77	C–C–C ring anti-symmetrical twist
ν_8	78	77	80	80	C–C–C ring symmetrical twist and carboxyl group torsion
ν_9	86	86	90	91	CH_2 anti-symmetrical twist
ν_{10}	90	91	91	91	Xanthene ring in-plane bending

Three vibrational modes' blue shifts are apparent in the FT spectra, as denoted by dashed-arrowed upwards lines in Fig. 5. The red ones connecting Figs. 5(b) and 5(a) represent the experimental results while the blue ones pointing from Fig. 5(d) to Fig. 5(c) refer to homologous calculation results. The phenyl ring torsion mode (ν_1) is located at 26 cm^{-1} (with largest Raman activity below 100 cm^{-1}) in the GSA & SE band FT power spectrum, and it turns into 29 cm^{-1} in the ESA band FT power spectrum, as shown by oblique upward red dashed lines. This matches well with the theoretical calculation result when shifting from 24 cm^{-1} to 27 cm^{-1} during S_0-to-S_1 transition, as exhibited by oblique upward blue

dashed line.

Other distinct modes' blue shifts also appear in the FT power spectra. First, the wag mode of the phenyl ring parallel to xanthene ring (ν_5) with a frequency of 49 cm^{-1} in the S_0 state only arises in the GSA & SE band FT power spectrum, while the same mode in S_1 state with a frequency of 57 cm^{-1} appears both in GSA & SE and ESA FT power spectra. This result coincides with the calculated change from 51 cm^{-1} to 58 cm^{-1} within the error range. Second, the calculated C–C–C ring anti-symmetrical twist vibration (ν_7) with a frequency of 72 cm^{-1} in S_0 state only appears in the GSA & SE band FT spectrum as indicated at 71 cm^{-1}, while the calculated same mode in S_1 state with a frequency of 75 cm^{-1} coupled with 80 cm^{-1} (78 cm^{-1} in S_0 state) vibration mode occurs in both of two FT spectra with frequencies of 77 cm^{-1} and 80 cm^{-1}.

The peaks at both 14 cm^{-1} and 20 cm^{-1} only appear on the two FT power spectra; however, the calculated results show that there is no molecular vibrational mode with frequency below 23 cm^{-1}, which demonstrates that none of them is derived from single molecular vibration but may originate from collective vibrations. The FT power spectrum at about 30 cm^{-1} appears in neither of the two states. and the FT power spectrum near 25 cm^{-1} in S_0 state may come from their relatively low Raman activity. In addition, the unexpected envelop occurs at 63 cm^{-1} in Fig. 5(a) may stem from low-frequency modes' coherent coupling in excited state between ν_1 (27 cm^{-1}) and ν_3 (38 cm^{-1}).

Through a comparative analysis between quantum chemical calculation and FT spectra of TG signal, it can be confirmed that the vibrational information in ground- and excited-state of $Rh101^+$ can be separated by BB-TG spectra and their FT power spectra at various wavelengths. Specifically, the FT spectrum in GSA & SE band contains the mixed dynamics of ground and excited state while excited state vibrational information is included only in ESA band.

Furthermore, according to the quantum chemical calculation, it is also found that the molecular configuration of $Rh101^+$ is transformed during the electronic transition from S_0 to S_1 state. In brief, the xanthene ring, phenyl and the carboxyl group show better coplanarity after electronic transition. Interestingly, the vibrational modes of $Rh101^+$ involving with phenyl and carboxyl group present relatively obvious changes during the electronic transition from S_0 to S_1 state; for instance, ν_1, ν_3, ν_5 and especially ν_6 shift 4, 8, 7, and 40 cm^{-1}, respectively. The other modes shift inconspicuously; for example, ν_2, ν_{10} shift less than 1 cm^{-1}, even the most remarkable mode (ν_7) only shift less than 3 cm^{-1} (the carboxyl group torsion in ν_8 is quite weak). The geometry change of $Rh101^+$ in S_1 state concentrates on phenyl and carboxyl group, and the results reveal that molecular configuration has a decisive influence on the frequency of the same vibrations.

5. Conclusions

Theoretical analysis based on double-sided Feynman diagrams indicates that the dynamics in GSA & SE overlapped band contains both ground and excited electronic states' vibrational information. Meanwhile, only excited electronic state vibrational coherence is contained in the ESA band. The TG experiment in which a broadband probe pulse with $Rh101^+$ is used as a target molecule is carried out. GSA & SE overlapping band and ESA band are both observed in the time-resolved TG spectra. After Fourier analysis at particular wavelengths in positive delay time range of the TG dynamics and comparing with quantum chemical calculation, the theoretical expectations are proven. Low-frequency vibrational modes of $Rh101^+$ in ground- and excited- electronic states are distinguished. Three vibrational modes with obvious blue shift are observed after the electronic transition. The results also reveal that the frequency of specific vibrational mode is seriously affected by the molecular structure and by the electronic states.

This work proves that the Fourier transform (FT) for TG transient at various wavelengths is an effective way to distinguish vibrational modes from different electronic states. This method shows good performance, even when the frequency of vibration mode is relatively low and the target molecule has strong fluorescence. Owing to its simple operation and relative high efficiency, this method can be generalized to more molecules.

References

[1] Basilevsky M V 1974 *Mol. Phys.* **28** 617

[2] Anelli P L, Spencer N and Stoddart J F 1991 *J. Am. Chem. Soc.* **113** 5131

[3] Murakami H, Kawabuchi A, Kotoo K, Masashi Kunitake A and Nakashima N 1997 *J. Am. Chem. Soc.* **119** 7605

[4] Golestanian R, Liverpool T B and Ajdari A 2005 *Phys. Rev. Lett.* **94** 220801

[5] Kukura P, McCamant D W and Mathies R A 2007 *Ann. Rev. Phys. Chem.* **58** 461

[6] Fork R, Greene B and Shank C V 1981 *Appl. Phys. Lett.* **38** 671

[7] Schmitt M, Knopp G, Materny A and Kiefer W 1997 *Chem. Phys. Lett.* **280** 339

[8] Brown E J, Zhang Q and Dantus M 1999 *J. Chem. Phys.* **110** 5772

[9] Materny A, Chen T, Schmitt M, Siebert T, Vierheilig A, Engel V and Kiefer W 2000 *Appl. Phys. B* **71** 299

[10] Kobayashi T, Du J, Feng W and Yoshino K 2008 *Phys. Rev. Lett.* **101** 037402

[11] Kobayashi T and Yabushita A 2009 *Chem. Phys. Lett.* **482** 143

[12] He P, Fan R, Chen D, Li X, Xia Y, Yu X and Yao Y 2011 *Opt. Laser Technol.* **43** 1458

[13] Liebel M and Kukura P 2013 *J. Phys. Chem. Lett.* **4** 1358

[14] Lincoln C N, Hayden J, Pour A G, Perlík V, Šanda F and Hauer J 2016 *Vib. Spectrosc.* **85** 167
[15] Ruhman S, Joly A G and Nelson K A 1987 *J. Chem. Phys.* **86** 6563
[16] Yan Y X, Jr E B G and Nelson K A 1985 *J. Chem. Phys.* **83** 5391
[17] Liebel M, Schnedermann C, Wende T and Kukura P 2015 *J. Phys. Chem. A* **119** 9506
[18] Wende T, Liebel M, Schnedermann C, Pethick R J and Kukura P 2014 *J. Phys. Chem. A* **118** 9976
[19] Shirley J A, Hall R J and Eckbreth A C 1980 *Opt. Lett.* **5** 380
[20] Mukamel S 1995 *Principles of nonlinear optical spectroscopy*, (Oxford: Oxford University Press)
[21] Pastirk I, Brown E J, Grimberg B I, Lozovoy V V and Dantus M 1999 *Faraday Discuss.* **113** 401
[22] Yu G Y, Song Y F, He X, Zheng X X, Tan D W, Chen J and Yang Y Q 2012 *Chin. Phys. B* **21** 043402
[23] Voehringer P and Scherer N F 1995 *J. Phys. Chem.* **99** 2684
[24] Venkateswarlu P, George M C, Rao Y V, Jagannath H, Chakrapani G and Miahnahri A 1987 *Pramana* **28** 59
[25] Frank A J, Otvos J W and Calvin M 1979 *J. Phys. Chem.* **83** 716
[26] Pereira E J N, Berberan-Santos M N, Fedorov A, Vincent M, Gallay J and Martinho J M G 1999 *J. Chem. Phys.* **110** 1600
[27] Saik V O G A A and Fayer M D 2004 *J. Chem. Phys.* **120** 9601
[28] Jiang L L, Liu W L, Song Y F, He X, Wang Y, Wang C, Wu H L, Yang F and Yang Y Q 2014 *Chem. Phys.* **429** 12
[29] Gaussian 03 R E, Frisch M J, Trucks G W, Schlegel H B *et al.* (eds.) 2004
[30] Laury M L, Carlson M J and Wilson A K 2012 *J. Comput. Chem.* **33** 2380
[31] Merrick J P, Moran D and Radom L 2007 *J. Phys. Chem. A* **111** 11683